

Spray-Coated Fluorine-Free Superhydrophobic Coatings with Easy Repairability and Applicability

Weici Wu,^{†,‡} Xiaolong Wang,[‡] Xinjie Liu,^{†,‡} and Feng Zhou^{*,†}

State Key Laboratory of Solid Lubrication, Lanzhou Institute of Chemical Physics, Chinese Academy of Sciences, Lanzhou 730000, People's Republic of China, and Graduate College of Chinese Academy of Sciences, Beijing 100083, People's Republic of China

ABSTRACT The present paper reports a very simple and low-cost fluorine-free superhydrophobic coating prepared by spray-coating metal alkylcarboxylates, for example, $\text{Cu}[\text{CH}_3(\text{CH}_2)_{10}\text{COO}]_2$, onto virtually any substrates. Superhydrophobicity with a static water contact angle of about 160° and a sliding angle of 5° was achieved from the proper precursor concentration. The advantages of the present approach include the cheap and fluorine-free raw materials, environmentally benign solvents, an industrial implementation method, and easy repairability and applicability so as to make a great application potential in practice. The hydrophobicity of coatings and the adhesion to water were found to be dependent on the surface morphology that was governed by the precursor concentrations from which coatings were prepared. The static wetting behavior of water droplets with different sizes gently deposited on the coatings was studied in more detail and correlated to theories, i.e., Wenzel's and Cassie's models. The results indicated that nanoribbon-textured coatings prepared from low precursor concentration (0.02 M) exhibited a transition from the metastable Cassie–Baxter state to the Wenzel state with increments in the droplet volume, and eventually droplets firmly stick to the surface even when the droplet was gently deposited on the surface. Surface coatings with dual roughness at both microscale and nanometer scale were formed as the concentration (0.04 M) was increased and conferred a stable Cassie state, even for increased droplet size and increased droplet deposit speed.

KEYWORDS: superhydrophobic coating • spray • repairability • Wenzel–Cassie transition

INTRODUCTION

In recent years, enormous contributions have been made to superhydrophobic surfaces that mimic the “lotus-effect” (1) as a typical example in nature for self-cleaning protection. The self-cleaning effect comes from the combination of special micro/nanocomposite (2) structures and natural low-energy materials such as the wax exudation of a plant. The research work on artificial superhydrophobic surfaces has been focused on two aspects, in which the creation of micro/nanostructured surfaces is particularly valued to increase the air fraction on surfaces so that even hydrophilic materials can be made superhydrophobic. Most of the fabrication strategy starts by the construction of micro/nanostructures on surfaces including light irradiation (3, 4), solvent evaporation (5), wetting chemical etching (6), plasma deposition (7), sublimation (8), a sol–gel method (9), chemical vapor deposition (10), high-temperature curing (11), and etching of engineering metals/alloys in long-chain alkanecarboxylate (12, 13) and ends up with modification with low-surface-energy materials such as perfluorochemicals. Nature uses a genetically formed scaffold and consecutively emitted simple waxlike materials to achieve superhydrophobicity,

and most of the natural superhydrophobic surfaces can be maintained very well by themselves in the environment. In the preparation of artificial superhydrophobic surfaces, the simple and low-cost fabrication approach is very crucial; however, its durability is also very important, in practice, but is rarely considered. Unlike the nature that can repair or reconstruct surfaces, manmade superhydrophobicities are almost weak to mechanical contact on the surface for their fine structures; what's more, they almost cannot be repaired automatically, which makes the artificial surfaces lose their “self-cleaning” function. This posts the key question regarding its application, can the benefits coming from superhydrophobicity compensate for the cost of a complicated fabrication approach? If not, what is the right way? It seems that the self-cleaning capability of artificial surfaces would even be difficult to afford with nature's way, i.e., via self-refreshing coatings. The alternative way would be to develop surface coatings with cheap materials, simple fabrication, and easy repairability. Actually, some simple methods such as spraying have been adopted to cater to those requirements of obtaining artificial superhydrophobic surfaces, which can even be commercially available now. For example, the super-water-repellent material HIREC, which can be sprayed to form coatings used in preventing the adhesion of snow, ice, and other substances besides water, has been developed by NTT Advanced Technology Corp. In this Communication, we report a real simple, low-cost, and nontoxic method to prepare superhydrophobic coatings

* To whom correspondence should be addressed. E-mail: zhouf@lzb.ac.cn.
Received for review March 3, 2009 and accepted July 6, 2009

[†] Chinese Academy of Sciences.

[‡] Graduate College of Chinese Academy of Sciences.

DOI: 10.1021/am900136k

© 2009 American Chemical Society

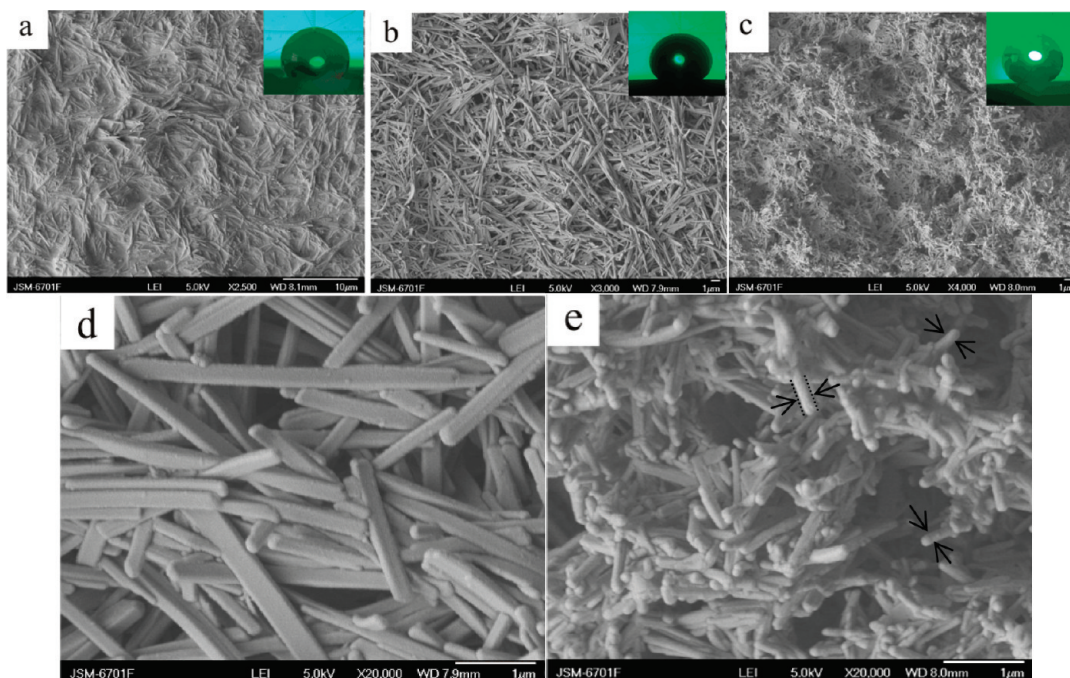


FIGURE 1. SEM morphology of the as-prepared copper dodecanecarboxylate coatings spray-coated at different concentrations, (a) 0.01 M, (b) 0.02 M, and (c) 0.04 M, and the shapes of the water droplets on these surfaces (the volumes of the water droplets are all 5 μL). (d and e) Magnified images of parts b and c, respectively.

made by spraying a alkanecarboxylate emulsion solution on virtually any substrates and curing at ambient environment, which if mechanically damaged just needs to be repaired by spraying, so it is a fairly cheap method so far with wide applicability. Interestingly, the hydrophobicity of this coating can be enhanced just by gradually increasing the precursor concentration, resulting in an enhanced roughness and a transition in its contact state with droplets occurring from the Wenzel model to the stable Cassie model, eventually corresponding to the evolution of surface micro/nanotextured structures.

EXPERIMENTAL DETAILS

The emulsion solution of $[\text{CH}_3(\text{CH}_2)_{10}\text{COO}]_2\text{Cu}$ with a concentration from 0.01 to 0.04 M in a mixed solvent of ethanol and water (1:1, v/v) was prepared first. Then the as-prepared emulsion was sprayed onto glass, aluminum, or other substrates with nitrogen gas (Figure S1 in the Supporting Information) and dried under room temperature and for 2–3 h at ambient temperature until the mixed solvent gradually evaporated. The thickness of the coatings was estimated in the range of 20–60 μm .

Scanning electron microscopy (SEM) images were taken by a JSM-5600LV SEM setup. X-ray photoelectron microscopy (XPS) analysis of the sample was performed on a VG Escalab 210 (VG Scientific) spectrometer with a Mg $\text{K}\alpha$ X-ray source (1253.6 V). The X-ray diffraction (XRD) pattern was recorded on a Philips X'Pert Pro (AMC, America) X-ray diffractometer in the 2θ range from 1° to 75° with Cu $\text{K}\alpha$ radiation ($\lambda = 0.1544 \text{ nm}$). Contact angles (CAs) and sliding angles of 5 μL water droplets on the coatings were measured with a CA-A contact angle meter at ambient temperature (CA-A, Kyowa Scientific Co. Ltd., Japan). The image of the droplet and dynamic movie were obtained by a digital camcorder (Sony, DSC-T700). Images were analyzed using video play software.

RESULTS AND DISCUSSION

The surface morphologies of the as-prepared coatings are clearly shown by the SEM images in Figure 1. The concentration of the Cu $[\text{CH}_3(\text{CH}_2)_{10}\text{COO}]_2$ emulsion plays a crucial role in determining the surface structure and wetting behavior. From Figure 1, it is seen that these rough coating surfaces composed of stacking clusters were stepwise formed by increases in the concentration. When the applied concentration of the emulsion was 0.01 M, the coating was constructed by sparse nanorods lying on the surface, as shown in Figure 1a. The coating was relatively smooth, with a low roughness, and its water advancing static CA was only $126 \pm 1.4^\circ$ (the CA image shown in the inset). A doubled concentration of 0.02 M resulted in a textured surface composed of nanoribbons (Figure 1b, coating b). It is seen from Figure 1d that the nanoribbons in coating b were almost all stacked in the horizontal direction, lying parallel to the substrate for most of the nanoribbons, although the lengths seem to be different. Most of these nanoribbons were about several micrometers in length and about 250–300 nm in width and relatively uniform (Figure 1d). The textured surface had an enhanced hydrophobicity, showing a water advancing CA of $140 \pm 2^\circ$. When the concentration was further increased to 0.04 M (coating c), the surface roughness was enhanced and a more complicated morphology containing binary micro/nanostructures (microscale papillae and nanoscale rods) was formed, which dramatically enhanced the roughness. A close view of the surface (see Figure 1e) shows that the surface was composed of numerous nanorods of about 100–150 nm diameter and they were almost vertically oriented, in contrast to that formed from a 0.02 M solution. The coating demonstrated a great water-repellent property with an advancing static CA

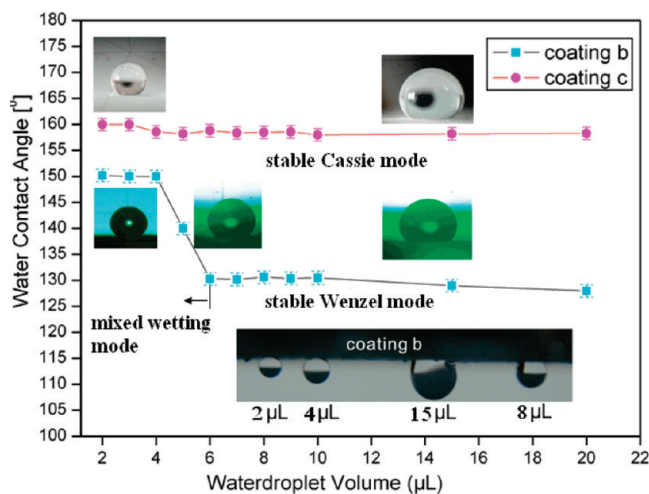


FIGURE 2. Relationship between the WCA and its volume on the as-prepared coatings b and c. The inset is a photograph of hanging water droplets with different sizes on coating b.

of $158 \pm 2^\circ$ and a low sliding angle of $5 \pm 1.4^\circ$. The copper alkanolate nanorods might have been formed via self-assembly in solution (14) and further oriented in the vertical direction during evaporation of the solvent. The XPS and Fourier transform IR (FTIR) spectra shown in Figures S2 and S3 (see in the Supporting Information) demonstrate that the stacking nanostructures of these coatings were composed of $\text{Cu}[\text{CH}_3(\text{CH}_2)_{10}\text{COO}]_2$. The small-angle-region diffraction pattern of the powder XRD (see Figure S4 in the Supporting Information) demonstrates that the as-prepared copper alkanolate has a layer structure with the same d spacing, as labeled with lines indexed to the interlayer spacing. Such a layer structure is analogous to that of $\text{CH}_3(\text{CH}_2)_{10}\text{COOAg}$ with a calculated d spacing value of 33.80 \AA (15). According to our experiment, the concentration is a crucial factor in the formation of nanomorphology of metal alkanolates probably by exhibiting different morphological assemblies in solution at different concentrations. The hydrophobicity/superhydrophobicity of these coatings (coatings b and c) even without further modification with low surface energy originates for two reasons: first, the copper alkanolates are intrinsically hydrophobic with the outmost long alkyl chains; second, the greatly enhanced roughness or the air/solid composite interface plays an important role. How is that different from coating c? Obviously, they have much larger pockets of air fractions than nanotextured surfaces including coating b. The air cushion largely contacting with the water droplet in the composite interface often greatly enhances the surface hydrophobicity (16–18).

Two contact models of water droplets on the rough surfaces were usually used to describe the wetting behavior of a surface, i.e., Wenzel's and Cassie's models, respectively (17, 19). Both contact ways can bring about the superhydrophobic state. Moreover, both states can coexist in the same rough surface (20–23). In Cassie's model, the water droplet is largely supported by air trapped between the water droplet and the surface, while Wenzel's model describes the cases where surface trapped air is expelled and the water droplet has direct contact with the surface. Water will pene-

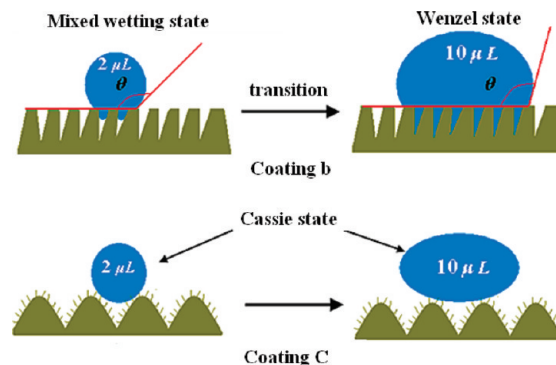


FIGURE 3. Schematic illustration of the wetting mode of droplets of different sizes on coatings b and c.

trate into the cavities on a textured surface and result in a decrease of the CA. The irreversible transition from Cassie's to Wenzel's models (21) is not desired for robust superhydrophobic surfaces. For the relatively smooth morphology formed at a concentration of 0.01 M in Figure 1a, the contact model is apparently in the Wenzel model, the advancing static CA is only $126 \pm 1.4^\circ$, and the water droplets could be tightly adsorbed onto this coating surface (high-contact-angle hysteresis). Upon a further increase of the concentration to 0.02 M (coating b), a nanotextured surface was formed where nanoribbons crossed into a dense network so that a considerable amount of air was trapped on the surface, which is expected to bring about Cassie's contact model, but actually causes a more complicated wetting mode. From Figure 2, it is clear that increasing the water volume from 2 to 20 μL on coating b led to a corresponding decrease in the advancing static CA from $151 \pm 1.2^\circ$ to $130 \pm 2^\circ$. Roughly, there were three stages for this variation, i.e., a stable superhydrophobic stage from 2 to 4 μL , a rapid drop stage from 4 to 6 μL , and a stable hydrophobic stage from 6 to 20 μL or even more. Meanwhile, the coating surface showed large CA hysteresis of at least 100° for water droplets of 5 μL . In contrast, coating c demonstrated excellent superhydrophobicity, and its high CAs would not change by increased pressure from the water droplet weight or external disturbance. The water CAs (WCAs) almost remained at a high value of about 160° despite the fact that the water volume changed from 2 to 20 μL . Moreover, all of these water droplets were easy to slide off the surface, implying very low hysteresis in contrast to that of coating b.

From the wetting and adhesion data, we can get some glue to the wetting modes on the two coatings. Despite its superhydrophobicity, coating b exhibited strong adhesive force and high hysteresis and apparently was in the pure Wenzel mode. However, the increased volume of the water droplet from 4 to 6 μL led to a sharp decrease of wetting from superhydrophobicity to general hydrophobicity, indicating a change of the contact mode between the droplet and the surface. Imaginably, when a tiny droplet as small as 2 μL was deposited on it, it penetrates a little into the microcavities at the bottom, so the CA remained as high as above 150° , while a small penetration would result in a strong release from the capillary and van der Waals forces compared to its self-gravity. An increased weight of the

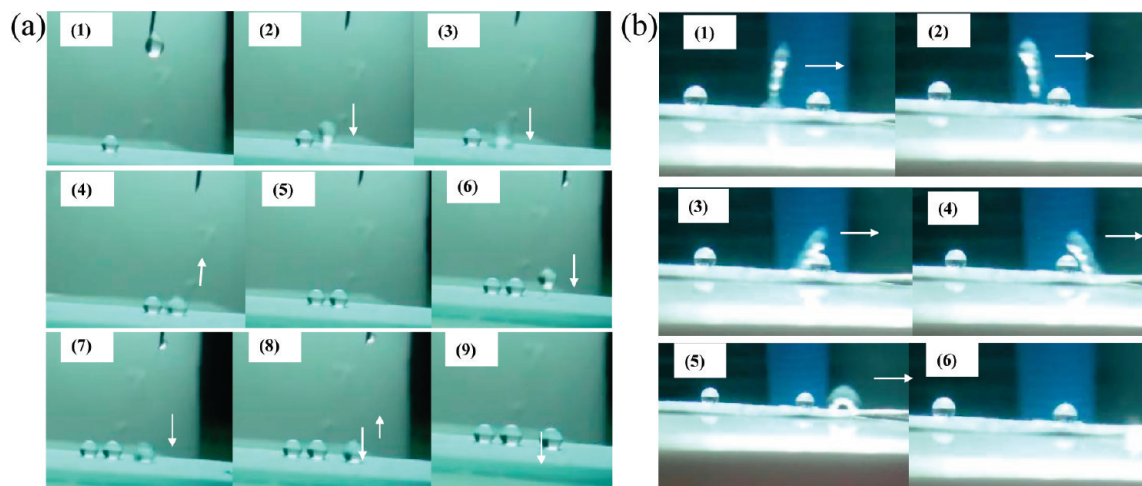


FIGURE 4. (a) Snapshots of water droplets of $10\ \mu\text{L}$ hitting the surface of coating b. Impact velocity = $0.545\ \text{m/s}$. (b) Snapshots of water droplets of $10\ \mu\text{L}$ falling at a height of about $80\ \text{mm}$ impacting the surface of coating c. Impact velocity = $1.25\ \text{m/s}$.

water droplet would lead to full wetting of the nanoribbon texture in the contact area because of an increase in the hydraulic pressure (24). The CA would not change too much after a critical pressure created by a $6\ \mu\text{L}$ droplet in this case. Therefore, the droplet on coating b was in a mixed wetting mode when the droplet was smaller than $6\ \mu\text{L}$ and a stable Wenzel mode. The wetting transition implies that the trapped air in coating b was actually in a metastable state and can be readily squeezed off. This transition can also be explained as a process to overcome the energy barrier of the composite metastable state to reach the thermodynamically favored Wenzel state (25–28). Coating c with binary micro/nanostructures shows a great air pocket in the composite interface of Cassie's contact model; thus, the deposited water droplet floated on the air cushion. When the volume of the water droplet increased from 2 to $10\ \mu\text{L}$, the water droplet was slightly flattened under gravity, but the CA values did not change much. The schematics of the contact modes on the two coatings and thus the induced CA change are shown in Figure 3.

The dynamic behavior of water droplets on superhydrophobic surfaces is of great importance in practical applications. Also, good superhydrophobicity with both high CAs and low sliding angles is always desired. To find the principle in designing the robust superhydrophobic surface, many researchers have studied the transition induced by the impact of a droplet on the patterned surface (29–31). Jung and Bhushan (32) investigated the effects of the impact velocity on the transition to patterned surfaces with different geometric parameters. Rioboo et al. (33) have tested the ability of the surface to bounce drops as a function of the drop size and drop impact velocity. However, the real superhydrophobic coatings, potentially applied to many fields such as self-cleaning of the architecture's wall, have not been examined on its robustness as to whether it can endure the rainy conditions with the impact of falling water droplets. If not, its ability to keep the architectural surface from fouling remains in question. In the following, the impact effects on this spray-coated surface were tested by water droplets with different velocities and sizes and were

used to further evaluate the wetting modes on the two coatings. First, the sliding behavior on inclined coatings was tested as a measure of the surface adhesive force to water. The movie1 in the Supporting Information indicated that coating b had a highly sticky property to the water droplet even on the inclined surface, further verifying the Wenzel contact model between the water droplet and the coating surface. In comparison, coating c was very repellent to a water droplet of even $10\ \mu\text{L}$. The water droplet could easily slide down when it was carefully deposited on the tilting surface. When it was thrown onto this coating, it bounced off immediately, implying the robustness of superhydrophobicity.

Furthermore, the dynamic behavior of droplets was observed on horizontal coatings b and c to find whether droplets bounced away from coating b and whether the transition from the Cassie–Baxter to Wenzel state occurred with the impact. Figure 4a (1–9) show the droplets hitting coating b. Water droplets of $10\ \mu\text{L}$ with a velocity of $0.545\ \text{m/s}$ pinned on this coating, just vibrating with no bouncing off. The results indicated that these droplets had a Wenzel contact model with coating b, and the hydrophobicity of coating b may not be enough from the view of practical application. Because the water droplets falling onto this surface with variable velocity mostly stick to the surface, the surface sticky force eventually further increases to liquids or waste. However, for coating c, the situation completely changed in its superhydrophobicity. Water droplets of $10\ \mu\text{L}$ falling with a velocity of $1.25\ \text{m/s}$ rebounded on coating c and moved from left to right in about $60\ \text{ms}$, as shown in Figure 4b (1–6). Obviously, the droplets hit the coating surface and formed a liquid–air–solid interface. In other words, droplets remained in the Cassie–Baxter model contact. We also measured the static WCAs of droplets after impact as a function of the impact velocity by taking droplets of 5 and $10\ \mu\text{L}$ as the probe liquid for coatings b and c, respectively. The results are shown in Figure 5. It is seen that, for coating c, after impact with 0.88 and $1.25\ \text{m/s}$ the advancing CAs slightly decreased. However, they still remained higher than 150° and the droplets could easily slide on this coating

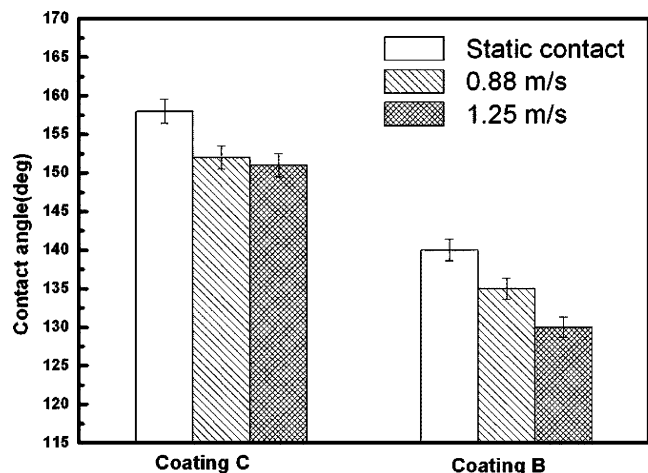


FIGURE 5. Impact effect on the WCAs.

surface. The trapped air remained in the composite interface between the impacting droplets and the surface, so the Cassie–Baxter model was preserved. Therefore, the coating was resistant to impact and exhibited good superhydrophobicity. However, when the droplets impacted coating b in some velocities, water was in all probability thrust into the nanocavities and drove away the trapped air. Eventually, an obvious decrease in the advancing CA occurred after impact and the surface showed a strong adhesion to water drops.

This reproducible coating can be applied to various substrates such as metal, glass, or even paper (see Figure 6a). The adhesion of coatings to substrates was tested by high-speed rotation of the coatings on a spin-coating machine. At the high-speed rotation of 4000 rps, the copper alkananoate coatings on the glass slide and aluminum plates remained with no loss. It can keep its superhydrophobicity for at least 6 months at atmosphere conditions, which shows its long-term stability. Other metal alkananoates with alterable metal or alkylcarboxyl have also been synthesized such as $\text{Cu}[\text{CH}_3(\text{CH}_2)_{12}\text{COO}]_2$ or $\text{Cd}[\text{CH}_3(\text{CH}_2)_{10}\text{COO}]_2$. All of these metal alkananoate coatings on various substrates show good superhydrophobicity (Figure 6).

There are some reports on making superrepellency to water or oil on metal surfaces using in situ generated metal alkananoates/perfluoroalkanoates (12, 13) or metal alkanethi-

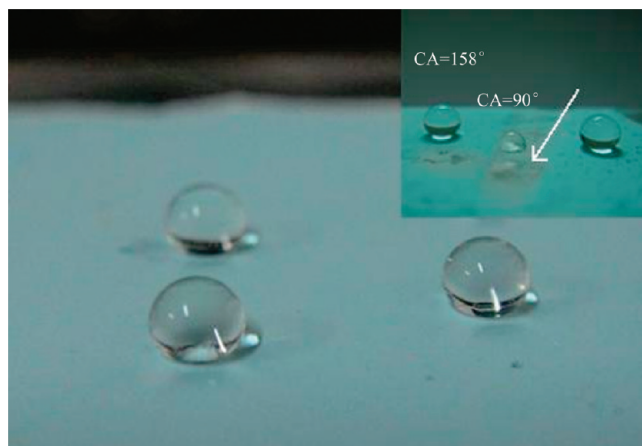


FIGURE 7. Photographs of water droplets on the as-prepared superhydrophobic surface with repairability by spraying. The inset is a copper alkananoate coating partly destroyed by mechanical scratching.

olates (16). These surfaces are limited to certain substrates and fragility, making it difficult to restore the superhydrophobicity upon surface damage. In our method, alkanecarboxylate can be used more conveniently and faster to construct a superhydrophobic coating when spray-coated from proper concentrations on various substrates including metal, glass, paper, etc. The cheap nontoxic coating materials and solvent and its simplicity in implementation make the strategy attractive for real applications. Regarding the real application, the surface wettability is actually very weak, especially upon contamination with hard contact. The stability of the “self-cleaning” function in nature is realized by the self-refreshment of surface coating materials, which is, however, rather difficult to implement artificially. However, this problem was rarely paid enough attention. Mechanical durability may be the biggest problem in that any mechanical scratch will dramatically affect the WCA value. The present coating can also be easily scratched because there is no strong chemical bonding to substrates. However, its repairability should be stressed from two aspects: first, repair is easily carried out by simple spraying and, second, the coating material is very cheap, allowing local repair at any time and almost any where. As shown in Figure 7, when the sprayed superhydrophobic coating over a large area was

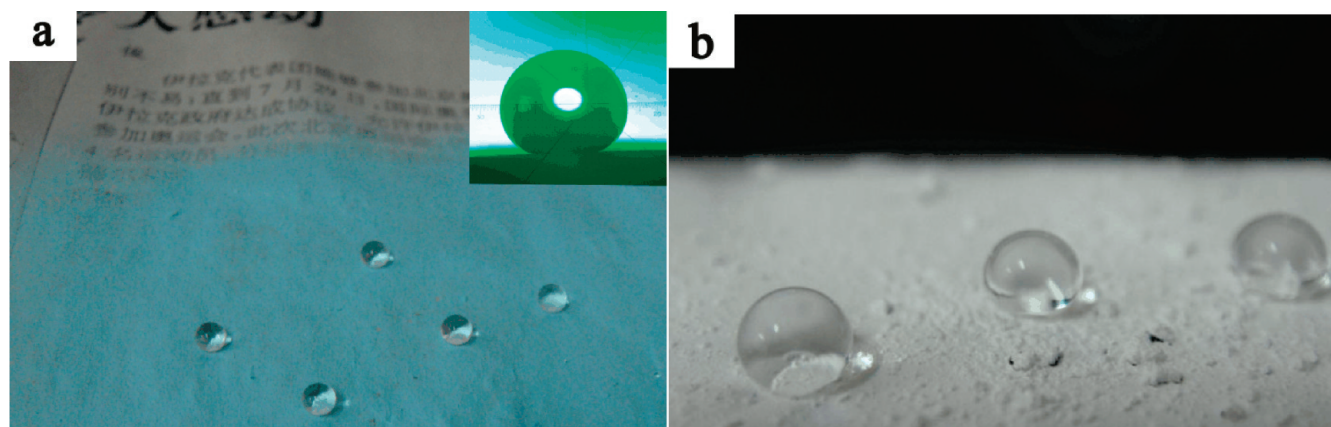


FIGURE 6. Water droplets sitting on as-prepared metal alkananoate superhydrophobic coatings: (a) $\text{Cu}(\text{CH}_3(\text{CH}_2)_{10}\text{COO})_2$ coating on newspaper; (b) $\text{Cd}(\text{CH}_3(\text{CH}_2)_{10}\text{COO})_2$ coating on a glass slide.

damaged in some area intentionally, a sharp decrease of its WCA from $158 \pm 2^\circ$ to about 90° was found in the inset image. To renew the superhydrophobic copper alkanolate coating, one just needed to carry out the spraying–curing process at room temperature once again directly on the wrecked surface. After evaporation of the water/ethanol mixed solvents for about 2 h, the reparative coating restored its good superhydrophobicity, as indicated in Figure 7. The easy reparability is expected to be highly demanded in the future for the real application of superhydrophobicity.

CONCLUSION

The intention of the present work is to discuss the requirement for the real applications of the widely reported superhydrophobicity and provides an as-simple-as-possible solution. The primary requirement of the application is the robustness of superhydrophobicity, easy reparability upon damage, and simple applicability. The strategy to make superhydrophobic coatings on various substrates by spraying metal alkanolates and curing at ambient environment can meet the requirement. The coating morphology can be optimized by controlling the precursor concentration to reach a binary micro/nanostructure and robust superhydrophobicity that was demonstrated via both the static and dynamic wetting studies. This superhydrophobic coating has good adhesion to various substrates such as metal, glass, paper, etc., and long-term stability when exposed to the environment. The superhydrophobic coatings are expected to have broad industry applications, for example, the self-cleaning of buildings and anticorrosion of metals especially at high humidity or in rainy conditions.

Acknowledgment. The work is financially supported by the “Top Hundred Talents” Program of CAS, “973” (Grants 2007CB607601), and NSFC (Grants 50835009 and 20804055).

Supporting Information Available: Experimental details and XPS and FTIR spectra for a copper alkanolate coating as well as its powder XRD pattern and movies of battery randomization. This material is available free of charge via the Internet at <http://pubs.acs.org>.

REFERENCES AND NOTES

- (1) Barthlott, W.; Neinhuis, C. *Planta* **1997**, *202*, 1.
- (2) Gao, X. F.; Jiang, L. *Nature* **2004**, *432*, 36.
- (3) Ichimura, K.; Oh, S.; Nakagawa, M. *Science* **2000**, *288*, 1624.
- (4) Feng, C.; Zhang, Y.; Jin, J.; Song, Y.; Xie, L.; Qu, G.; Jiang, L.; Zhu, D. *Langmuir* **2001**, *17*, 4593.
- (5) Erbil, H. Y.; Demirel, A. L.; Avci, Y.; Mert, O. *Science* **2003**, *299*, 1377.
- (6) Zhang, X.; Shi, F.; Yu, X.; Liu, H.; Fu, Y.; Wang, Z. Q.; Jiang, L.; Li, X. Y. *J. Am. Chem. Soc.* **2004**, *126*, 3064.
- (7) Chen, W.; Fadeev, A. Y.; Hsieh, M. C.; Öner, D.; Youngblood, J.; McCarthy, T. J. *Langmuir* **1999**, *15*, 3395.
- (8) Nakajima, A.; Fujishima, A.; Hashimoto, K.; Watanabe, T. *Adv. Mater.* **1999**, *16*, 1365.
- (9) Tadanaga, K.; Morinaga, J.; Matsuda, A.; Minami, T. *Chem. Mater.* **2000**, *12*, 590.
- (10) Li, S.; Li, H.; Wang, X. B.; Song, Y.; Liu, Y.; Jiang, L.; Zhu, D. *J. Phys. Chem. B* **2002**, *106*, 9274.
- (11) Luo, Z.; Zhang, Z.; Hu, L.; Liu, W.; Guo, Z.; Zhang, H.; Wang, W. *Adv. Mater.* **2008**, *20*, 970.
- (12) Wang, S.; Feng, L.; Jiang, L. *Adv. Mater.* **2006**, *18*, 767.
- (13) Xi, J.; Feng, L.; Jiang, L. *Appl. Phys. Lett.* **2008**, *92*, 053102.
- (14) Yuan, Z. W.; Lu, W. J.; Liu, W. M.; Hao, J. C. *Soft Matter* **2008**, *4*, 1639.
- (15) Binnemans, K.; Deun, R.; Thijs, B.; Vanwelkenhuysen, I.; Geuens, I. *Chem. Mater.* **2004**, *16*, 2021.
- (16) Chen, S.; Hu, C.; Chen, L.; Xu, N. *Chem. Commun.* **2007**, *10*, 1919.
- (17) Cassie, A. B. D.; Baxter, S. *Trans. Faraday Soc.* **1944**, *40*, 546.
- (18) Tao, Y. T. *J. Am. Chem. Soc.* **1993**, *115*, 4350.
- (19) Wenzel, R. N. *Ind. Eng. Chem.* **1936**, *28*, 988.
- (20) Lafuma, A.; Quéré, D. *Nat. Mater.* **2003**, *2*, 457.
- (21) Patankar, N. A. *Langmuir* **2003**, *19*, 1249.
- (22) Patankar, N. A. *Langmuir* **2004**, *20*, 7097.
- (23) Quéré, D.; Lafuma, A.; Bico, J. *Nanotechnology* **2003**, *14*, 1109.
- (24) Zheng, Q.-S.; Yu, Y.; Zhao, Z.-H. *Langmuir* **2005**, *21*, 12207.
- (25) He, B.; Patankar, N. A.; Lee, J. *Langmuir* **2003**, *19*, 4999.
- (26) Barbieri, L.; Wagner, E.; Hoffmann, P. *Langmuir* **2007**, *23*, 1723.
- (27) Neinhuis, C.; Barthlott, W. *Ann. Bot.* **1997**, *79*, 667.
- (28) Jin, M. H.; Feng, X. J.; Sun, T. L.; Zhai, J.; Li, T. J.; Jiang, L. *Adv. Mater.* **2005**, *17*, 1977.
- (29) Richard, D.; Clanet, C.; Quéré, D. *Nature (London, U.K.)* **2002**, *417*, 811.
- (30) Reyssat, M.; Pépin, A.; Marty, F.; Chen, Y.; Quéré, D. *Europhys. Lett.* **2006**, *74*, 306.
- (31) Bartolo, D.; Bouamrine, F.; Verneuil, E.; Buguin, A. *Europhys. Lett.* **2006**, *74*, 299.
- (32) Jung, Y. C.; Bhushan, B. *Langmuir* **2008**, *24*, 6262.
- (33) Rioboo, R.; Voué, M.; Vaillant, A.; De Coninck, J. *Langmuir* **2008**, *24*, 14074.

AM900136K